Modelling of a Solar Photovoltaic Power Supply for a Wireless Access Point in a Rural Area

Thomas Djotio Ndié[1(✉)], Alphonse Tabué Kamga[1], and Karl Jonas[2]

[1] University of Yaounde 1, National Advanced School of Engineering of Yaounde, Yaoundé, Cameroon
tdjotio@gmail.com, alphonse.kamga08@gmail.com
[2] University of Applied Sciences, Hochschule Bonn-Rhein-Sieg, Sankt Augustin, Germany
karl.jonas@h-brs.de

Abstract. The digital divide remains a major concern for rural areas in developing countries in general and for sub-Saharan Africa in particular. It is particularly characterized by the unavailability of energy resources on which the functioning and operation of network connectivity infrastructure depends. The constraints of availability of electrical energy, coupled with the difficulty of access, make it difficult to implement relevant and sustainable digital solutions in these hard-to-reach areas. We propose in this article, a model for solar photovoltaic power generation that allows for autonomous and continuous operation of a wireless access point (WAP) in areas where access to electrical power is difficult. Our approach first consists of designing the system and mathematically modeling the photovoltaic solar panel and the BUCK series chopper, as well as the P&O type MPPT control for the solar panel' maximum power point tracking. Finally, we simulate the operation of the system for appreciating its behavior in a possible real situation. For this final point, before the simulation process, we realized the system's global diagram consisted of the solar generator, adaptation stage (provided with the MPPT control of type P&O) and battery park. This simulation allowed us to study the behavior of the system in normal conditions but also in particular conditions reflecting the environment in which it will be deployed. The results of the simulation are satisfactory and allowed us to validate the model we proposed. We have successfully designed a solar photovoltaic power supply for the WiABox 2507 that takes into account all its energy constraints.

Keywords: wireless access point · photovoltaic generator · MPPT · DC-DC converter series · Pertub&Observ algorithm

1 Introduction

In a computer network, a wireless access point (WAP) is an intermediate device that uses radio waves for allowing wireless devices to access a wired network or the Internet. The access point can be a stand-alone gateway router directly connected to a network. It can also be directly integrated as part of the router itself. To use it in remote locations, it should be self-sufficient in electrical power, which would give it the distinction of being mobile. The source of electrical energy that powers it could be renewable, for example; in most cases it is a solar power supply.

A. Sere et al. (Eds.): AFRICOMM 2023, LNICST 587, pp. 113–130, 2025.
https://doi.org/10.1007/978-3-031-81570-6_8

Telecommunications/ICTs are slowly progressing in rural and remote areas of developing countries, especially in those with special public policies, initiatives and subsidies. In general, telecommunication/ICT services, such as basic telephony, short message services, videoconferencing and internet services, is almost absent [1, 2] in sparsely populated rural areas. Provided a range of digital applications and services to people in rural areas can significantly improve their economy, quality of life and reduce inequality. Examples include telephone and short message service (SMS), Internet services, e-(business, health, finance, culture, banking, learning, inclusion, government), telework, and Internet of Things/M2M services. In the current context where the whole world has been stricken by the CORONA VIRUS pandemic that affects the school system especially in rural areas, the proximity network services are an excellent tool to improve the living conditions in these areas.

This is one of the motivating reasons why the inception of the WiABox 2507 project [3, 4]. WiABox 2507 is a multi-band, broadband wireless access technology capable of operating in a dedicated frequency range to provide reliable and sustainable ubiquitous services in rural areas, mainly in developing countries [4]. Its objective is to realize an autonomous and sustainable wireless access point to provide proximity network services in a community. The constraints for a WiABox 2507 access node are as follows:

- Compatibility with WiBACK (Fraunhofer FOKUS' wireless backhaul technology) & current IEEE 802 standards
- Based on open infrastructure (soft and hardware) and integrates emerging paradigms like SDN, SDR, TV White Space.
- Ability to operate on a range of frequencies instead of dedicated frequencies.
- Enable the development of resilient, persistent and sustainable wireless mesh networks.
- Serve as optimized end-user support for critical and emergency remote applications for unconnected areas.
- Be able to operate without interruptions in areas with insufficient or no access to electrical power.

It is on this last point that this paper is focused. The goal is to propose a WAP that is autonomous in electricity, mobile, and therefore suitable for remote areas. The objectives are: (1) To model, design and realize a solar power system perfectly adapted to the WiABox 2507 technology to allow its use in remote areas. (2) Provide network support for the operation of IoT-based systems. (3) Develop low-cost equipment to make the system affordable. (4) Provide equipment that is easy to maintain, install, and use.

2 Modeling of the WiABox 2507 Power Supply System

2.1 System Description

Our photovoltaic power system for the WiABox 2507 will consist of a solar panel that converts solar energy into electricity, a rechargeable battery that stores the energy produced and a charge controller that controls the charge of the battery. When the WiABox 2507 is connected to this system, it uses the energy stored in the battery to operate.

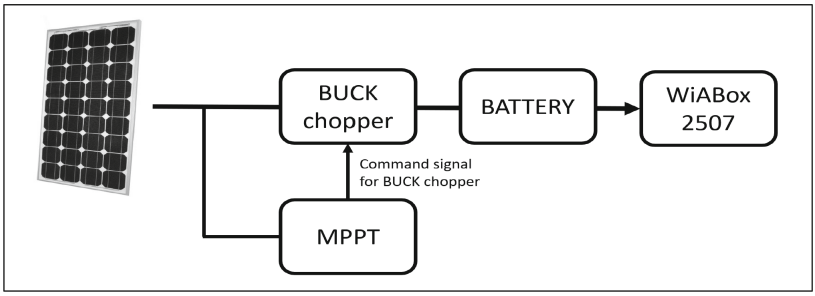

Fig. 1. Block diagram of the WiABox 2507 power supply system

Figure 1 shows the general structure of our autonomous photovoltaic system [5]. This structure is composed of four blocks: the solar panel, the charge controller (with a "Buck" type chopper and its MPPT control), the battery and the load, which in our case is the WiABox 2507.

The WiABox 2507 works with 12 V and calls for a maximum DC current of 02 amps when fully charged, that is a maximum power of 24 W. In order to guarantee an efficient, reliable and long lasting energy source it is recommended to adopt an autonomy of 04 days for our solar photovoltaic power system [6]. For that, we will need: (a) a monocrystalline solar panel of 210 watts-peak; (b) a storage battery of 72 A-hours (Ah) to have an autonomy of the system in average of 04 days; (c) a regulator/controller of load delivering a maximum current of 15 amperes (A), to easily convey the current coming from the solar panel for charging. The charge controller is equipped with a DC-DC converter, which is controlled by a pulse width modulation signal with a maximum power point tracking algorithm (MPPT). The system diagram is shown in Fig. 1.

2.2 Modeling of the Photovoltaic Solar Panel

A photovoltaic solar panel is composed of one or more photovoltaic solar cells whose function is to convert the power of solar radiation into electrical power. The cell behaves like a solar cell with a series resistance (Rs) and a shunt resistance (Rsh). These resistors will have some influence on the characteristic I = f(V). The series resistance represents the internal resistance of the cell. It mainly depends on the resistance of the semiconductor used, the contact resistance of the collector gates and the resistivity of these gates [7].

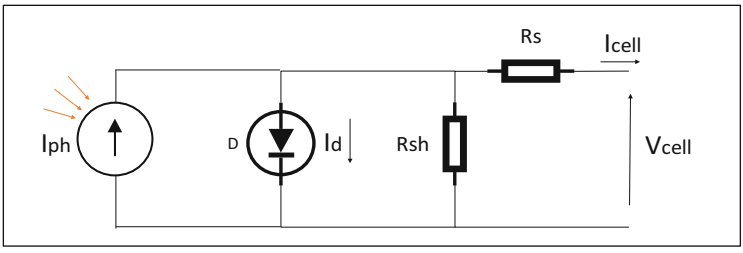

Fig. 2. Electrical diagram of a photovoltaic cell

The shunt resistance is due to a leakage current at the junction, it depends on the way it was made (Fig. 2);

This model uses a current generator to model the incident luminous flux, a diode for the phenomena of polarization of the cell and two resistors (series and shunt) [7] for the losses. This model is said to have five parameters, these parameters are the photo-current (Iph), the saturation current (I0), the ideality factor of the junction (A), the series resistance (Rs) and the shunt resistance (Rsh).

The physical study of a photovoltaic cell [8] allows us to obtain the current equation of the load:

$$I_{cell} = I_{ph} - I_d - I_{Rsh} \tag{1}$$

I_{cell}: Current delivered by the photocell.
I_{ph}: Photo current.
I_d: Current of the diode.
I_{Rsh}: Shunt current.

The resistance (Rsh) is higher so we can neglect the current IRsh so the equation is written:

$$I_{cell} = I_{ph} - I_d \tag{2}$$

We can deduce the current delivered by a cell:

$$I_{cell} = I_{ph} - I_0\left[\exp\left(\frac{q(V_{cell} + R_S I_{cell})}{N_S AKT} - 1\right)\right] - \frac{V_{cell} + R_S I_{cell}}{R_{Sh}} \tag{3}$$

With:

q [C]: Charge of the electron (1.602. 10–19 C).
Ns: Number of cells connected in series.
A: Ideality constant of the junction ($1 < A < 2$).
K [J/K]: Boltzmann constant (1.3805 .10–23 J/K).

The equations described above cannot represent the I-V characteristic of a PV module since they are specific to a single PV cell that represents the basic element of the panel, so we introduce the module-specific equation:

$$I_{PV} = N_p I_{ph} - N_p I_0\left[\exp\left(\frac{q(V_{cell} + R_S I_{cell})}{N_S AKT}\right) - 1\right] - N_p \frac{V_{cell} + R_S I_{cell}}{R_{sh}} \tag{4}$$

With Ns the number of cells connected in series in a module and, Np the number of cells connected in parallel in a module.

The characteristics of the solar photovoltaic panel that we will use are:

- Maximum power: 210 Wp
- Open circuit voltage: 32.5 V
- Maximum power point voltage: 28.3 V
- Short circuit current: 8.22 A
- Current at maximum power point: 7.41 A

– Operating temperature: −40 °C to +85 °C
– Efficiency: 15.44%.

- **Influence of temperature**

Temperature has a considerable influence on the behavior of the photovoltaic cell [9] and thus on its efficiency. This influence is mainly reflected by a decrease in the generated voltage (followed by a very slight increase in current). Figure 3 below shows the current-voltage (I-V) (a) and power-voltage (P-V) (b) characteristics of a photovoltaic module for one level of sunlight and several levels of temperature:

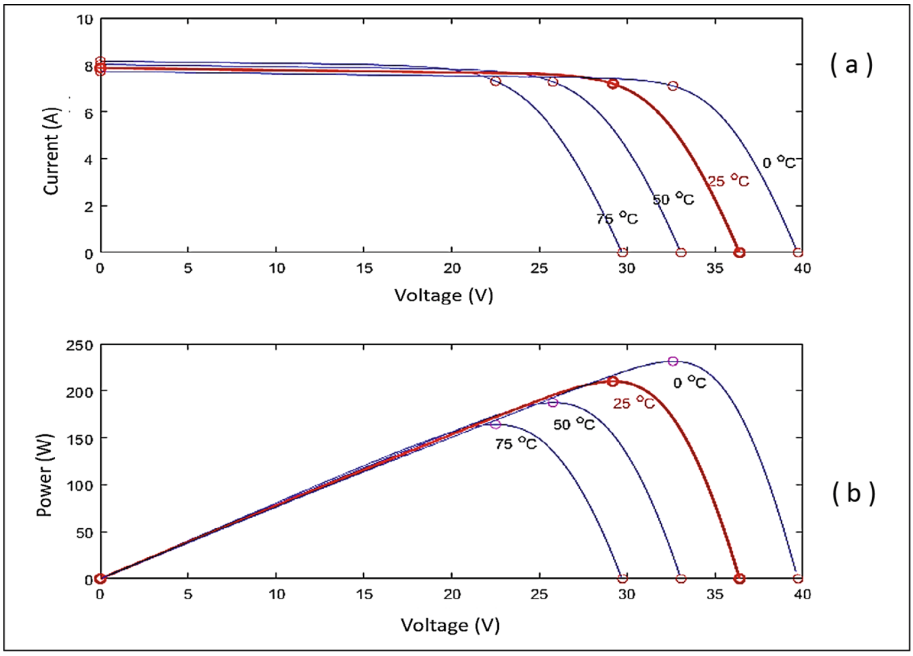

Fig. 3. (a) Influence of temperature on the current-voltage characteristic and (b) the power-voltage characteristic

We note a loss current of an order of magnitude estimated at 2.3mV/°C/cell. The short-circuit current increases slightly with the cell temperature (about 0.05% per degree Celsius).

- **Influence of solar radiation**

Here illustrated Fig. 4, we have varied the values of the sunlight level, kept the temperature constant, then, we have plotted the current-voltage (I-V) (a) and, power-voltage (P-V) (b) characteristics corresponding to each value. Photovoltaic cells exploit the photoelectric effect to produce direct current by absorption of solar radiation. This effect allows cells to directly converting the light energy of photons into electricity through a semiconductor material carrying electrical charges [10]. The efficiency of a

photovoltaic cell or module is the ratio between the electrical energy produced by this cell or module and the light energy received on the corresponding surface [11]:

$$n[\%] = Pproduced[kW]/Pincident[kW]$$

Therefore, the actual efficiency varies continuously, particularly depending on the incident solar energy [12]. The brightness has a considerable influence on the performance of the cells. As shown in the graph in Fig. 4, the current increases proportionally with the irradiance (Fig. 4.a), while the open circuit voltage varies very little (Fig. 4.b). Thus, the greater the cloud cover, the lower the current generated.

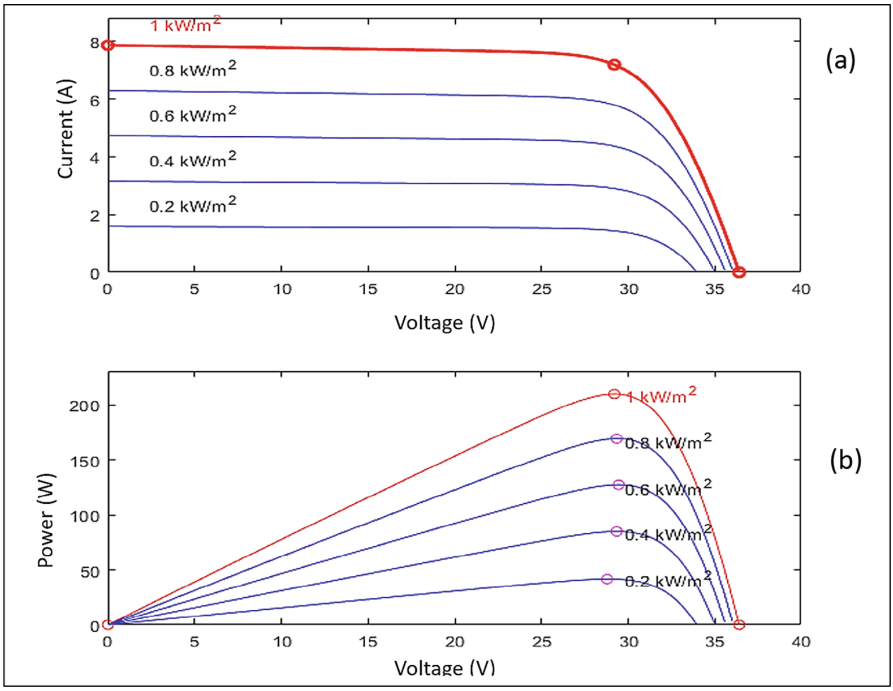

Fig. 4. (a) Influence of solar radiation on the current-voltage characteristic and (b) the power-voltage characteristic

From Eq. (4) we establish the Simulink model of the photovoltaic generator represented by the following Fig. 5:

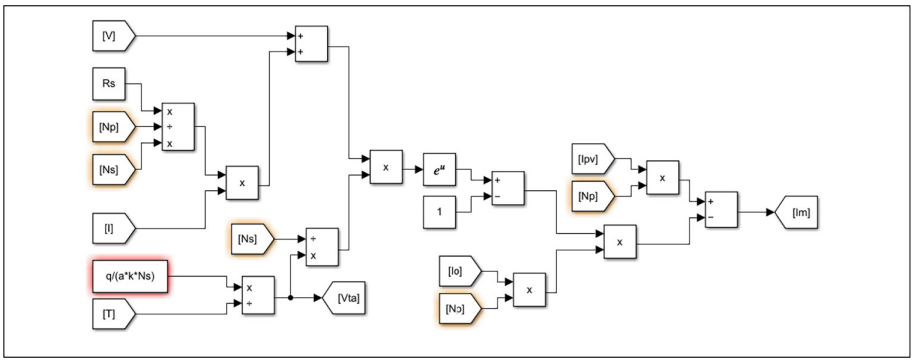

Fig. 5. Simulink model of the solar panel

2.3 Modeling the BUCK Chopper

A photovoltaic generator has non-linear current-voltage characteristics with a maximum power point (MPP) [1]. These characteristics depend on several parameters, the most important of which are the illumination level and the temperature of the photovoltaic cells. Moreover, depending on the characteristics of the load on which the GPV is delivering, we can find a very high discrepancy between the potential power of the photovoltaic array and the one actually transferred to the load in direct connection mode.

In order to extract the maximum power available at each moment at the terminals of the photovoltaic generator, and to transfer it to the load, the technique used classically is a matching stage between the photovoltaic generator and the load. There are two types of charge controllers: the PWM (Pulse Width Modulation) controller and the MPPT (Maximum Power Point Tracking) controller. We will use, for this work, the MPPT controller, which has a much higher efficiency than the PWM controller because, this stage plays the role of interface between the solar panel and the load. In addition, it has the advantage of ensuring, by a control action, the transfer of the maximum power supplied by the generator so that it is as close as possible to the maximum power available.

There are mainly three types of DC-DC converter: (a) the BUCK chopper used when the load voltage is lower than the voltage delivered by the solar panel, whose role is to convert its input voltage into a lower output voltage and keep it constant. (b) The BOOST chopper, used when the load voltage is higher than the voltage delivered by the solar panel, whose role is to convert its input voltage into a higher output voltage and keep it constant. (c) The BUCK-BOOST chopper used when the load voltage is lower or higher than the solar panel voltage, its role is to maintain the output voltage constant either by raising or by lowering the input voltage. The choice of one of these three choppers depends on the needs of the load in terms of voltage and current, as well as the specificities of the solar system. For our case, the BUCK and BUCK-BOOST chopper are indicated. The BUCK chopper has the advantage of a very good conversion efficiency, low electromagnetic noise, simplicity of the electronic circuit and a relatively low realization cost [13]. Nevertheless, the BUCK-BOOST chopper is more complex to realize, has a higher electromagnetic noise and is much more expensive. Our choice is therefore the BUCK chopper.

The BUCK chopper is a series type transistor DC-DC converter. The BUCK chopper consists of capacitors, inductor, diode and switch. It is designed for a power of 180 W corresponding to the nominal values I = 15 A, V = 12 V. Figure 6 shows the ideal circuit of the series chopper:

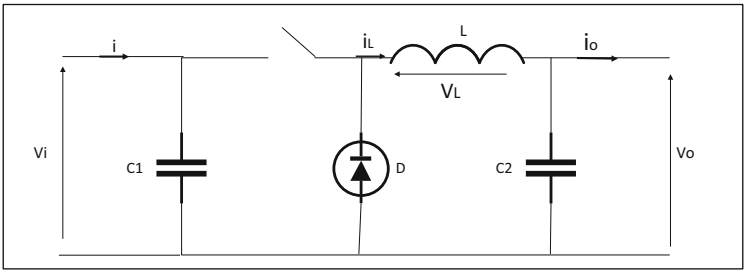

Fig. 6. Ideal circuit diagram of the series chopper

We note α, the duty cycle of the pulses that drive the switch and, *Te* the period of the pulses. Typically, the switch is a MOSFET or IGBT transistor, which are semiconductor devices in the "blocked-saturated" mode.

When the switch is closed for the duration αTe, a current flows through the circuit, but does not pass through the diode since it is inversely biased. The switch is driven at the switching frequency $fe = 1/Te$. The source *Vi* supplies power to the load and the inductor. During the time $t\varepsilon[\alpha Te, Te]$ the switch opens and the energy stored in the inductor drives the current flow in the freewheeling diode. The voltage across it is therefore zero.

- **Mathematical equivalent model**

In order to know the real behavior we have to make the representation of the equivalent circuit by the two states of the switch and then to draw the mathematical model linking the input/output variables. Figure 7 shows the equivalent circuit diagram of a devolving converter (series DC-DC converter) with the switch closed, while Fig. 8 represents the devolving converter with the switch open for $(1-\alpha)Te$.

When we apply Kirchhoff's law to the above circuit, we get the following equations:

$$\begin{cases} i_{c1}(t) = C\frac{dV_i(t)}{dt} = i(t) - i_L(t) \\ i_{c2}(t) = C_2\frac{dV_o(t)}{dt} = i_L(t) - i_o(t) \\ V_L(t) = L\frac{di_L(t)}{dt} = V_i(t) - V_o(t) \end{cases} \tag{5}$$

The system of Eqs. (6) is deduced from Fig. 7 above.

$$\begin{cases} i_{c1}(t) = C\frac{dV_i(t)}{dt} = i(t) \\ i_{c2}(t) = C_2\frac{dV_o(t)}{dt} = i_L(t) - i_o(t) \\ V_L(t) = L\frac{di_L(t)}{dt} = V_o(t) \end{cases} \tag{6}$$

We therefore present a model that must faithfully reproduce the operating sequences and simulate both continuous and discontinuous conduction, and especially the transition

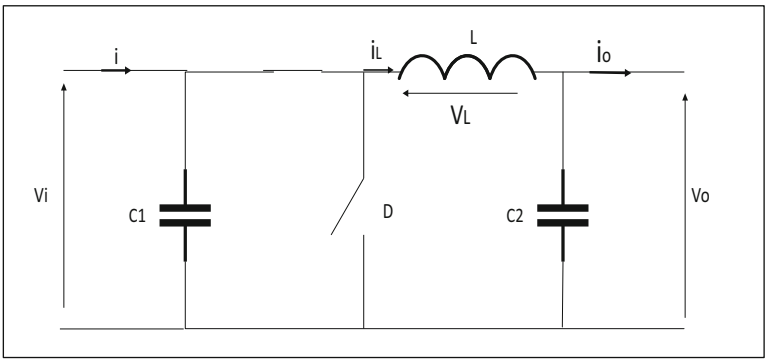

Fig. 7. Electrical diagram of the BUCK chopper in "closed" mode

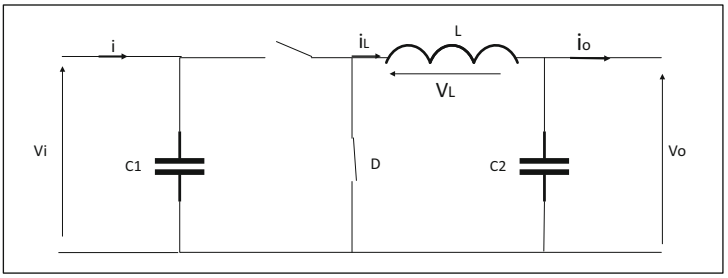

Fig. 8. Electrical diagram of the BUCK chopper in "open" mode

from one to the other [14]. For this, the nullity of the current *iL* must be verified during *toff* ; and if it occurs, the current must be maintained at zero until the beginning of the next period when it must increase again.

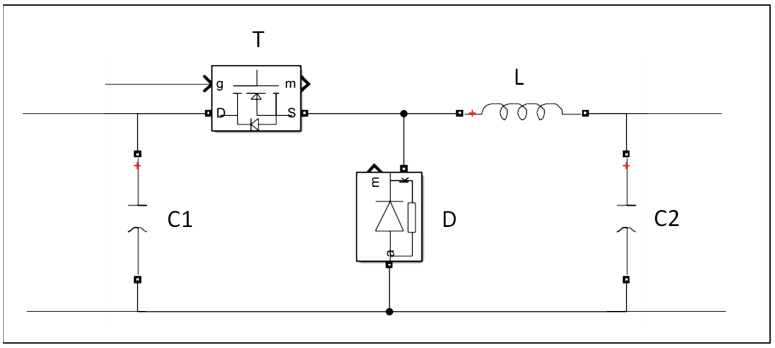

Fig. 9. Simulink model of the BUCK chopper

The Matlab-Simulink model proposed for this case precisely uses this detection of the current nullity. The identification of the conduction type is done by checking the

nullity of the sum of the control signal K and the current iL. For continuous conduction, this sum is never zero, whereas for discontinuous conduction, this sum is zero between ßT and T. When the nullity of this sum is detected, a switch is switched in order to cancel the variation of the current iL and thus to maintain zero until the beginning of the next period. On the other hand, all models used for all components are relatively real. For example, the switch and diode models have a series resistance and leakage inductance, while the capacitor and inductor models have a series resistance. The simulation model of the BUCK chopper developed for this application is given, under the Simulink software, by Fig. 9 above. This simulation model is quite realistic because it takes into account the imperfections of the components it contains.

2.4 Modeling the MPPT Control Algorithm

There are several MPPT control algorithms, the choice of one of these algorithms depends on the specific requirements and constraints of the project. In the case of a simple PV installation, the "Pertub and Observe" (P&O) algorithm is an effective and economical choice [15]. This method is based on using a feedback loop to adjust the input voltage of a DC-DC converter to find the maximum power point of the solar panel. The principle of the Perturbation and Observation method is to perturb the generator's VPV voltage by a small amount around its initial value and to analyze the behavior of the resulting PPV power variation [16]. If a positive increment of the VPV voltage results in an increase of the PPV power, it means that the operating point is to the left of the maximum power point. If, on the contrary, the power decreases, it implies that the system has exceeded the MPP [17]. A similar reasoning can be done when the voltage decreases. Among the advantages of the P&O algorithm are its simplicity (thus easily implemented using microcontrollers), its high reactivity to variations in solar irradiance, its robustness and reliability [18].

Figure 10 shows the flowchart of the P&O algorithm as it is to be implemented in the control microprocessor. Its Simulink model is shown in Fig. 11.

The P&O electronics determine, from the externally imposed setpoints and the measurements taken from the PV generator and the loads, the conduction and blocking sequence of the switch and elaborate the logic signals necessary for its control according to the type of converter used. In the case of the PWM control, the switch state is varied at each rate that does not depend on the way the quantities of the systems interconnected by the power electronic converter evolve, this rate being essentially fixed according to the switching speed.

Knowing that any switching is equivalent to changing the potential of a system terminal seen as a current source by connecting it to another system terminal seen as a voltage source, the control by pulse width modulation (PWM) will thus consist in choosing a switching frequency of the switch and, to fix within the switching period, the conduction intervals of the switches connected to a terminal of the "current source", according to a reference signal which corresponds to the desired potential for this terminal. In digital form, this type of control is achieved by fixing the conduction intervals of the various switches on each period or each half-period of modulation, as shown in Fig. 12.

The output of the comparator can be generated as a rectangular voltage modulated in width (variable duty cycle: PWM signal) [19]. This is the result of the comparison

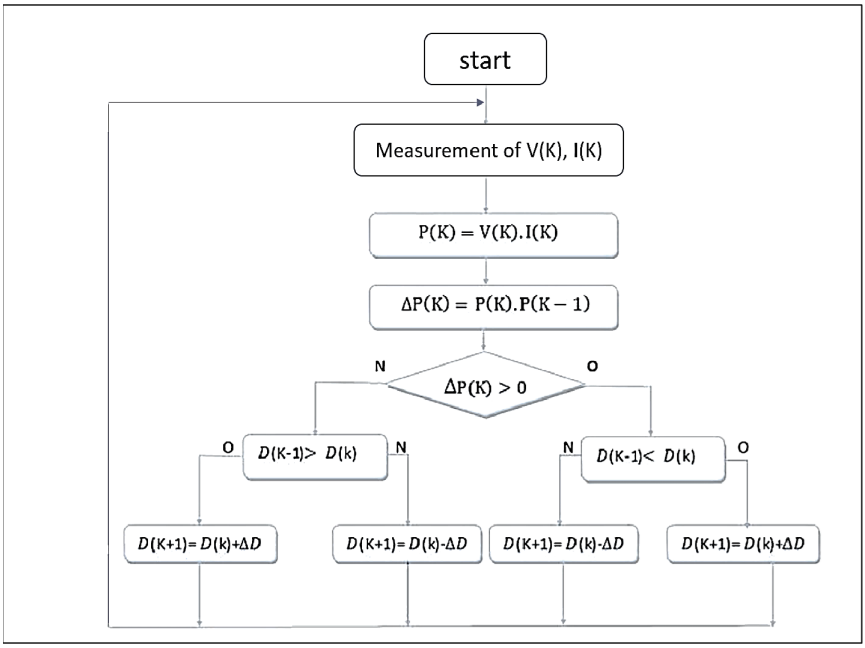

Fig. 10. Flowchart for finding the maximum power point using the P&O method.

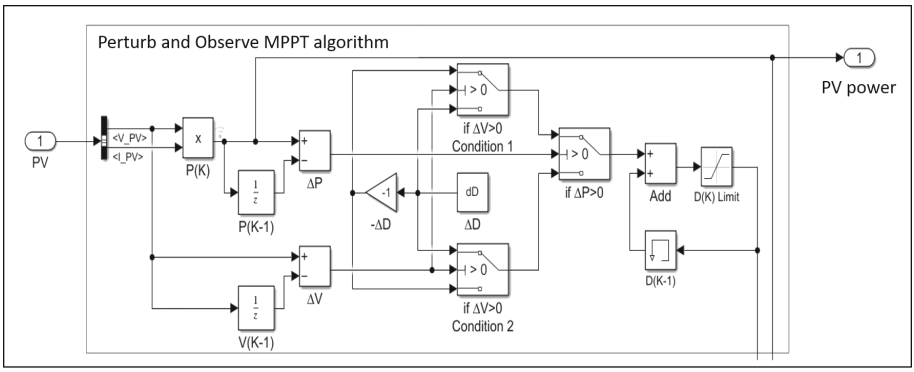

Fig. 11. Simulink model of the P&O algorithm

between the signal at the output of the integrator (Vref) and the one generated by a triangular generator with a frequency fixed by the converter operation. As the voltage Vref increases (decreases), the duty cycle α increases (decreases). The variations of the voltage Vref induce, for a given illumination and temperature, the displacement of the operating point on the power-voltage characteristic [19].

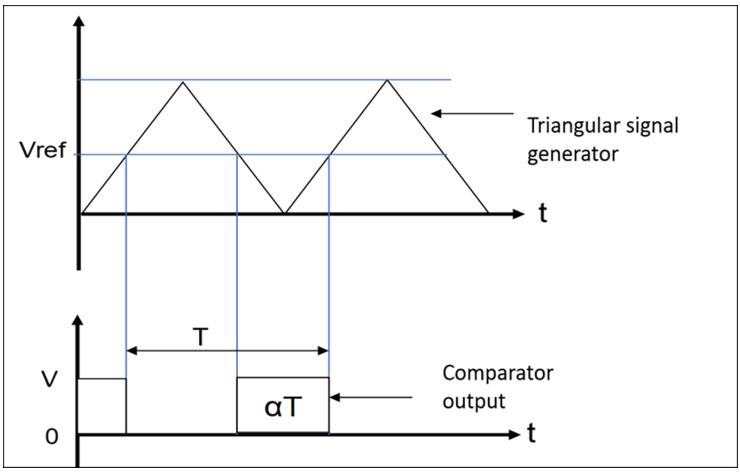

Fig. 12. Square-wave signal generation at the output of the comparator

3 Simulation and Analysis of Results

3.1 Overall System Diagram

Figure 13 represents the global schematic of our photovoltaic system; it is composed of a photovoltaic module with a power of 210 W-peak, a lithium-ion battery with a capacity of 72 A-hours (Ah) and a series chopper (BUCK) controlled by a P&O MPPT algorithm.

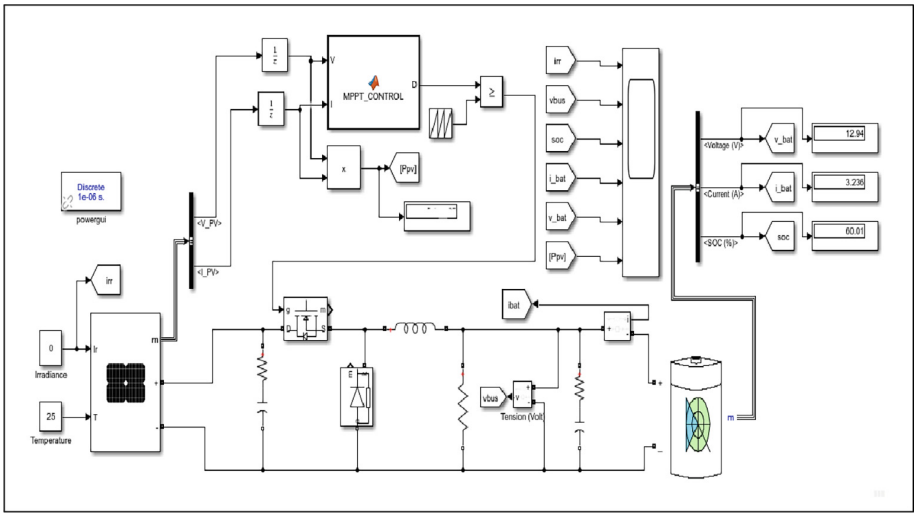

Fig. 13. Overall diagram of the Wiabox power system

To perform the simulation we used the mathematical model of all components of the WiABox 2507 power system. After having made the schematic of Fig. 13 and filled in the different values of the components, we started the simulation of our system.

3.2 Simulation Results

Several parameters must be taken into account to define the solar power supply required to cover an energy need. Apart from the choice of technology, the inclination and orientation of the solar panel, the temperature above the solar panel and the solar irradiation must be taken into account. The operation and profitability of a solar panel remains closely related to the rate of sunlight and the heat produced by the sun. In practice, the light intensity is the most important element in the operation and efficiency of a photovoltaic solar panel, more important than the heat. For the simulation of the system, we will study the behavior of the power system as a function of solar irradiation.

To carry out our simulation, we have considered a sample reflecting a variation of the solar irradiation in time. The Fig. 14 presents the curve of evolution of the sunshine in the time; we will use it for our simulation.

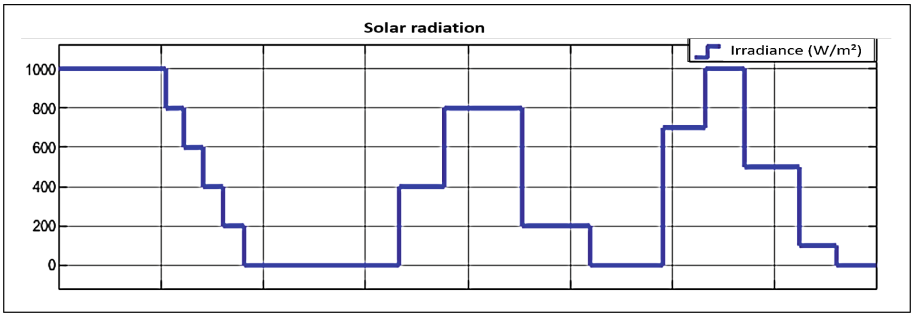

Fig. 14. Solar irradiance variation curve

Figure 14 illustrates a scenario representing the variation, in time and at constant temperature (25 °C), of the solar irradiation in a given location, reflecting a real case.

In Fig. 15 we can see the variation of the power of the photovoltaic solar panel as a function of the illumination. This is the power curve produced by the solar panel and transferred to the load through the charge controller. We can see that the controller constantly trying to extract the maximum power from the solar panel due to the many variations of the sunshine level. This is made possible thanks to the efficiency of the "Pertub & Observ" algorithm.

By zooming in on the plot of the power from the solar panel extracted by the charge controller, we can see the efficiency of the P&O algorithm, which tracks the point of maximum power to be extracted from the solar panel. We also observe that the response time of the algorithm following an abrupt change in the sunlight level is very favorable; it is around 0.025 s as shown in Fig. 16. Even under unfavorable weather conditions, the charge controller, using the P&O algorithm, always seeks to extract the maximum power from the solar PV array.

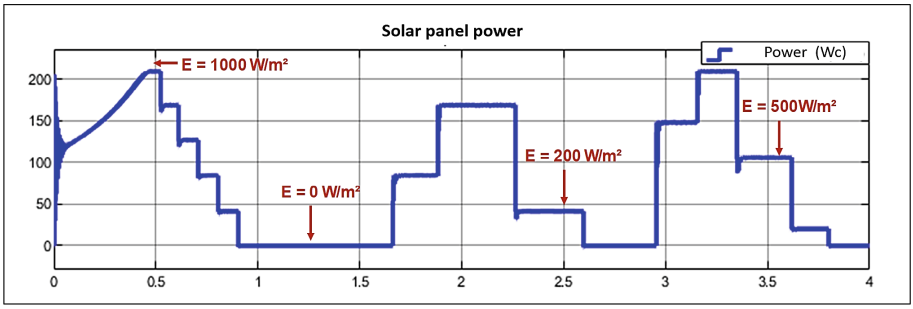

Fig. 15. Power of the solar photovoltaic panel

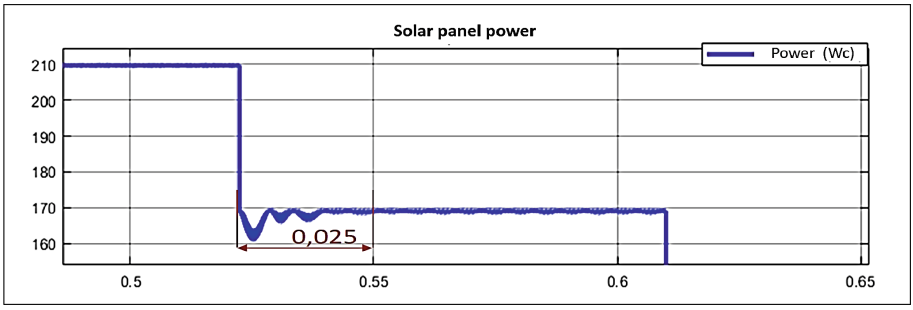

Fig. 16. Zoom on the curve of the power from the solar panel

Figure 17a shows the variation of the output voltage of the BUCK chopper as a function of the input power coming from the solar PV panel and the latter depends on the solar irradiation (Fig. 14). Figure 17b shows the variation of the voltage at the terminals of the battery supplied by the charge controller as a function of the amount of sunlight. We can see that Fig. 17a and Fig. 17b are identical; this is because the battery is directly connected to the charge controller, so they are equipotential.

The battery state of charge (SoC) is a relative measure of the amount of energy stored in a battery, defined as the ratio of the battery's charge at a certain time to its total capacity [20]. Accurate state-of-charge estimation is important because battery management systems use it to inform the user or the system itself of the remaining capacity until the next recharge to: (a) ensure proper battery operation; (b) implement control strategies and; (c) maximize battery life.

For the simulation, we used a Lithium-ion battery with 60% charge; Fig. 18 shows the result of the simulation of the charge and discharge of the battery as a function of the power from the solar panel (depending on the variation of sunshine). We notice that when the voltage at the terminals of the regulator is sufficient (i.e. higher than the voltage at the terminals of the battery bank), the battery is charged provided that its charge rate at this moment is not 100%. In the opposite case (the voltage at the terminals of the charge controller is lower than that at the terminals of the battery bank), the battery supplies energy to the load and to the controller, so naturally at this moment it discharges. This

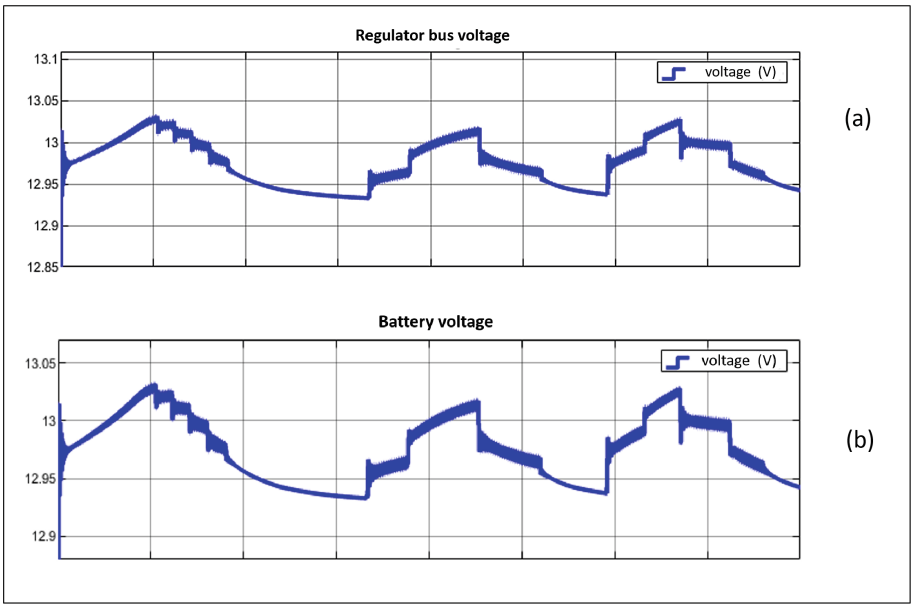

Fig. 17. (a) Variation of the output voltage of the BUCK chopper and (b) the battery voltage

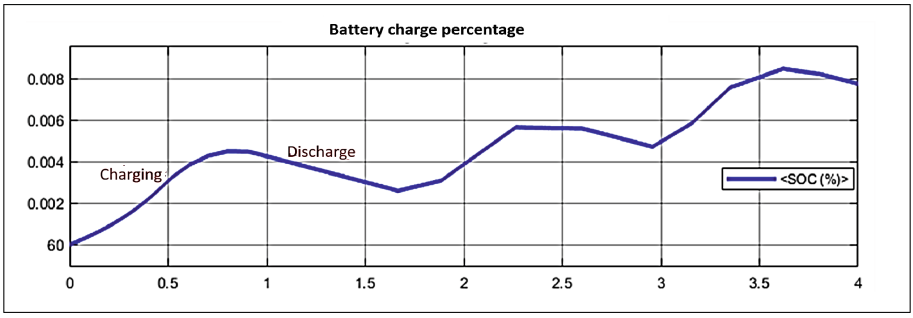

Fig. 18. Battery state of charge

second case occurs when the power from the solar generator is insufficient due to the level of sunlight.

The battery need to be recharged in order to store energy and release it when needed. Figure 19 shows the variation of the battery current as a function of sunshine (Fig. 14). We can see that this curve records negative and positive values; in fact, when the battery is in "CHARGE" mode, its current is negative, whereas when the battery is in "DISCHARGE" mode, its current is positive.

In Fig. 20, we see three zones (zone 1, zone 2 and zone 3). The zones 1 and 2 describe a phenomenon of regulation of the current of the battery following a brutal variation of this last due to the variation of the power of the solar generator (consequence of the

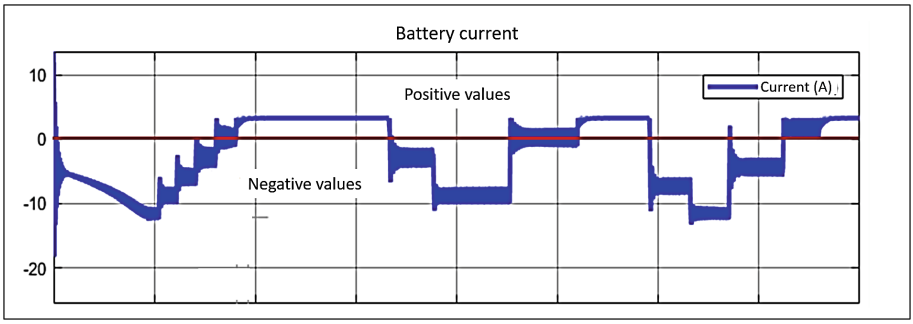

Fig. 19. Battery current as a function of solar radiation

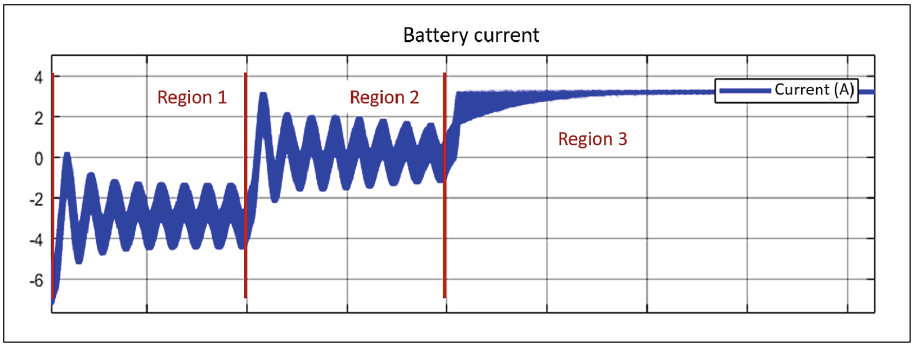

Fig. 20. Zoom on the battery current plot

variation of the sunning). We observe, on the zone 3, a stabilization of the current of the battery towards a fixed value.

4 Conclusion

This paper presents the design of a system that provides uninterrupted autonomous power to a wireless access point (WiABox 2507) in areas where electrical power is not readily available. The proposed solution integrates a power generation system operating through a P&O algorithm and a serial DC-DC converter. The objective of this approach was to improve the stability and efficiency of the system. To this end, the P&O algorithm was implemented in a BUCK converter and simulations with MATLAB software were done to validate the proposed model and demonstrate its efficiency.

Considering the requirements concerning the service continuity with respect to the availability of electrical energy at any time, this system is able to completely ensure this function even when the weather conditions are unfavorable. This system is designed to be used in various climatic environments (variation of temperature and humidity), for that, we could improve this work by studying the effects of the temperature on the

performance of our power system; in particular at the level of the solar panel and battery park.

References

1. Dragomir, T.L., Petcut, F.M. et al.: Maximum power point determination for a photovoltaic panel using a Simulink model. In: 4th International Workshop on Soft Computing Applications (2010)
2. Ko, G., Routray, J.K., Ahmad, M.M.: ICT infrastructure for rural community sustainability. Community Dev. **50**(1), 51–72 (2018)
3. Djotio, T., Jonas, K.: Open-source firmware customization problem: experimentation and challenges. In: Intelligent Computing, pp. 306–317 (2019)
4. Djotio, T., Jonas, K.: A pedagogical approach for developing a firmware from open source code: case of WiAFirm, an OpenWRT-based firmware for WiABox appliance. Wiabox 2507 project initiative, step1: specification. Tandem Workshop Dakar, Sénégal - 15–16 March 2016
5. Abouda, S., Nollet, F., Chaari, A., Essounbouli, N., Koubaa, Y.: Direct torque control of induction motor pumping system fed by a photovoltaic generator. In: 2013 International Conference on Control Decision and Information Technologies (CoDIT) (2013)
6. Nazaripouya, H., Wang, Y., Chu, P. et al.: Optimal sizing and placement of battery energy storage in distribution system based on solar size for voltage regulation. In: 2015, IEEE Power & Energy Society General Meeting, pp. 1–5 (2015)
7. Sene, M., Samoura, A., Diouf, S., Diao, A., Mbow, C.: Electrical modeling of a silicon photovoltaic solar cell: comparative study of models characterizing the photovoltaic solar cell. Open J. Appl. Sci. **13**, 1787–1795 (2023)
8. Dey, B.K., Khan, I., et al.: Mathematical modelling and characteristic analysis of solar PV cell. In: IEEE 7th Annual (2016)
9. Fesharaki, V.J., Dehghani, M., et al.: The effect of temperature on photovoltaic cell efficiency. In: Proceedings of the 1st International Conference on Emerging Trends in Energy Conservation – ETEC; Tehran, Tehran, Iran, 20–21 November 2011
10. Ramalingam, K., Indulkar, C.: Chapter 3 - solar energy and photovoltaic technology. In: Distributed Generation Systems, Butterworth-Heinemann (2017)
11. Zhang, T., Wang, R.: High efficiency plants and building integrated renewable energy systems. In: Handbook of Energy Efficiency in Buildings, Butterworth-Heinemann (2019)
12. Chegaar, M., Hamzaoui, A., et al.: Effect of illumination intensity on solar cells parameters. In: TerraGreen 13 International Conference - Advancements in Renewable Energy and Clean Environment (2013)
13. Baharudin, N.H., Mansur, T.M.N.T., et al.: Performance analysis of DC-DC Buck converter for renewable energy application. In: Journal of Physics: 1st International Conference on Green and Sustainable Computing, 25–27 November 2017
14. Lang, Y., Ge, X., Gu, R., Zhang, Y.: The closed-loop design for buck chopper circuit. In: International Conference on Circuits, Devices and Systems (ICCDS) 5–8 September 2017
15. Hilali, A., Mardoude, Y., Ben Akka, Y., El Alami, H., Rahali, A.: Design, modeling and simulation of perturb and observe maximum power point tracking for a photovoltaic water pumping system. Int. J. Electr. Comput. Eng. (IJECE) (2022)
16. Ram, J.P., Babu, T.S., Rajasekar, N.: A comprehensive review on solar PV maximum power point tracking techniques. Renewable Sustain. Energy Rev. **67**, 826–847 (2017)
17. Piegari, L., Rizzo, R.: Adaptive perturb and observe algorithm for photovoltaic maximum power point tracking. IET Renewable Power Gener. **4**(4), 317–328 (2010)

18. Subudhi, B., Pradhan, R.: A comparative study on maximum power point tracking techniques for photovoltaic power systems. IEEE Trans. Sustain. Energy **4**(1), 89–98 (2012)
19. Kim, S.-H.: Pulse width modulation inverters. In: Electric Motor Control, DC, AC, and BLDC Motors, pp. 265–340, Butterworth-Heinemann (2017)
20. Hamdi, A., Behnam, M., Saeid, J., Amir, R., Ehsan, D.: Chapter 7 - Energy storage systems. In: Distributed Generation Systems, Design, Operation and Grid Integration, Butterworth-Heinemann, pp. 333–368 (2017)